Int J Environ Res
DOI 10.1007/s41742-017-0050-2

RESEARCH PAPER

Utilization of Hydrogel–Fungus Composites as Absorbents for Removal of Textile Dyes from Aqueous Media

Tuba Ersen Dudu[1] · Duygu Alpaslan[1] · Yusuf Uzun[2] · Nahit Aktas[1]

Received: 22 April 2017 / Revised: 4 September 2017 / Accepted: 8 October 2017

Abstract Three different environmentally friendly new composite hydrogels were synthesized and utilized as absorbents for removal of toluidine blue (TB), alizarin red S (AR), and gallocyanine (G) dyes from aqueous media. The homo and co-hydrogels were synthesized via redox polymerization technique from 2-acrylamido-2-*methyl*-1-propane sulfonic acid sodium salt (AMPS) and 3-acrylamidopropyl-trimethyl ammonium chloride (APTMACl). *Polyporus squamosus* (Huds.) *Fr.* [*P. squamosus* (Huds.) *Fr.*] fungus was utilized as the bio-part of the composite hydrogels. The effects of pH, contact time, and initial dyes concentrations on the absorption of composite hydrogels were investigated in sequence. It was concluded that Freundlich isotherm model was the best-fitted ones through the computation of the experimentally observed data for common isotherms models such as Freundlich and Langmuir. The maximum absorption of TB by p(AMPS)-*P. squamosus* (Huds.) *Fr.*, of AR by p(APTMACl)-*P. squamosus* (Huds.) *Fr.*, and of G by p(APTMACl)-*P. squamosus* (Huds.) *Fr.* composite hydrogels were obtained to be 40.9, 31.3, and 36.7 mg/g, respectively. In addition, kinetic studies were carried out for all composite hydrogels and absorbed dyes to obtain the absorption behaviors of studied dyes. They were generally fitted well to a pseudosecond-order kinetic model, while TB dye absorption on the p(AMPS)-*P. squamosus* (Huds.) *Fr.* composite hydrogel fitted a pseudofirst-order kinetic model. The obtained data were compared with the literature and it is indicated that absorption capacities of both anionic and cationic composite hydrogels were considerable for utilization.

Keywords Anionic hydrogel (AMPS) · Cationic hydrogel (APTMACl) · *Polyporus squamosus* (Huds.) *Fr.* · Textile dyes · Absorption · Wastewater

Introduction

Pollutants from industries such as textile, printing, plastic, food, paper, pharmaceutical, cosmetic, and leather tanning are rather rich in dye and they are non-biodegradable, complex organic molecules, and even carcinogenic. Therefore, the discharges of these pollutants to the nearest especially water sources cause of environmental pollution in water and soil (Mahanta et al. 2008; Dong et al. 2013; Wang et al. 2010; Yagub et al. 2014). These pollutants' recovery through conventional physicochemical techniques such as separation and pre-concentration techniques is rather expensive and not eco-friendly. Therefore, biotechnological approaches have gained considerable importance as an alternative tool in the recent years (Iyer et al. 2005; Soylak et al. 2006; Vijayaraghavan et al. 2005; Akbari et al. 2015). Microorganisms by the ability of a large part of metabolic adaptability have shown resistance to different dye species including textile wastes, and many of them have the potential to remove dyes from aqueous solution. Both living and non-living biological biomass can be used as an effective dye and heavy metal collector, but the use of dead biomass is favored, since it is easy to handle; processes are growth independent and possess no harm while

✉ Nahit Aktas
naktas@yyu.edu.tr

[1] Engineering Faculty, Department of Chemical Engineering, Yuzuncu Yil University, 65080 Van, Turkey

[2] Faculty of Pharmacy, Department of Professional Pharmaceutical Sciences, Yuzuncu Yil University, 65080 Van, Turkey

Published online: 17 October 2017

using pathogenic strains (Pal et al. 2006). Consequently, biosorption is a popular technique that utilizes living/non-living biological materials for the removal of dyes. Among the most promising biomaterials studies, fungi are found to be very efficient and economically important (Pal et al. 2006; Vijayaraghavan et al. 2005).

Researches in the field of environmentally benign processes have revealed that in need of new kind of materials for removal of undesired contaminants from wastewaters (such as acrylamide/maleic acid hydrogels (Saraydın et al. 2001), alginate/poly aspartate hydrogels (Jeon et al. 2008), Coir pith activated carbon (Santhy and Selvapathy 2006), and activated carbon (Al-Degs et al. 2008). Recently, numerous approaches have been studied for the development of cheaper and more effective absorbents containing functional polymers or polymers/composite mixture for removal of a variety of pollutants (Ozay et al. 2011; Sahiner et al. 2011). Hydrogels and their composites are some of the most utilized materials among these approaches (Dong et al. 2013). Hydrogels as the crosslinked hydrophilic polymers are soft, flexible, and versatile materials and they can absorb large quantities of water and swell (Ho and McKay 1999; Sahiner et al. 2006, 2014; Alpaslan et al. 2014; Sahiner 2009). In addition, due to the functional groups in their basis chain, hydrogels can remove large quantities of dye forms and metal ions (Dong et al. 2013). Thus, both cationic hydrogel (APTMACl) and anionic hydrogel (AMPS) (a type of polymeric absorbent) have a high absorption capacity due to the fact that they show selectivity towards dye forms such as cationic and anionic. Fungi are abundant in nature and cheaper and they can be absorbed to different dye forms. Hydrogels can quite increase absorption capacities to different dye forms.

The objective of this study was to synthesize both cationic and anionic new composites from hydrogels and fungus. The composite hydrogels were synthesized from AMPS and APTMACl monomers via redox polymerization technique, while *Polyporus squamosus* (Huds.) *Fr.* fungus was utilized as the bio-part. In the absorption studies, various parameters such as the initial dyes concentrations, pH, and contact time were investigated. In addition, kinetic studies were carried out for the absorption of TB, AR, and G dyes by the prepared composite hydrogels. Freundlich isotherm was the best-fitted model among the isotherms that are commonly processed.

Experimental

Materials and Analysis Methods

3-acrylamidopropyl-trimethyl ammonium chloride (APTMACl) (75 wt%), 2-Acrylamido-2-*methyl*-1-propansulfonic acid sodium salt (AMPS) (50 wt%), toluidine blue (TB) ($C_{15}H_{16}ClN_3S.0.5ZnCl_2$), alizarin red S (AR) ($C_{14}H_7NaO_7S$), and gallocyanine (G) ($C_{15}H_{13}ClN_2O_5$) were purchased from Sigma-Aldrich, and *N*, *N*′-methylene bisacrylamide (MBA) (99%), *N*, *N*, *N*′, *N*′-tetramethylethylenediamine (TEMED) (99%), and ammonium persulfate (APS) (98%) were purchased from Merc. All reagents were of analytical grade or highest purity available and used without further purification. Natural *P. squamosus* (Huds.) *Fr.* fungus was collected from Yüksekova Territory in Hakkari Region, Turkey. The deionized water (DI water) was obtained from 18.2 MΩ cm (Millipore Direct-Q3 UV). The pH measurements were carried out with a Thermo Scientific pH meter. Ultraviolet spectroscopy (UV–Vis, Optizen POP, Korea) was used to quantify absorbed amount the of TB, AR, and G dyes during absorption studies.

Synthesis of Composite Hydrogels

First of all, naturally obtained fungi were ground and sieved to obtain the desired particle size (below 150 μm), dried in an oven at 40 °C for 24 h, and stored in desiccators for further utilization. Then, the composite hydrogels, which were p(AMPS-co-APTMACl)-*P. squamosus* (Huds.) *Fr.*, p(APTMACl)-*P. squamosus* (Huds.) *Fr.*, and p(AMPS)-*P. squamosus* (Huds.) *Fr.* were synthesized via redox polymerization technique (Alpaslan et al. 2014). Briefly, 1.5 mol% of MBA was dissolved in AMPS monomer, and the mixture was added to APTMACl with an equal amount to AMPS (1:1 mol ratio) and mixed thoroughly. Thereafter, 0.025 g of *P. squamosus* (Huds.) *Fr.* was added to the mixture. Then, 20 μL TEMED was added to the fungus hydrogel mixture, and the initiator solution APS (1 mol% of total monomer) in 100 μL water was added to the reaction mixture. The reaction mixture was mixed carefully for approximately 1 min and transferred into plastic straws with 5 mm diameter and allowed to polymerize and crosslink to complete the reaction at ambient temperature for approximately 1 hour. Then, composite hydrogels were removed from the plastic straws, cut into 6 mm-long cylinders, and cleaned by placing in DI water for 72 h. The composite hydrogels were washed with fresh water every 8 h to remove unreacted species, which were a monomer, polymer, crosslinker, fungus, and initiator. After the cleaning procedure, composite hydrogels were dried in an oven at 40 °C to a constant weight and kept in sealed containers for further studies (Sahiner and Alpaslan 2014; Ersen Dudu et al. 2015). The other composite hydrogels were synthesized by the similar procedure.

Characterization and Swelling Behavior of the Composite Hydrogels

The FT-IR analysis of composite hydrogels was completed with Fourier Transform Spectroscopy (FT-IR, Thermo Nicolet iS10 FT-IR Spectrometer, USA) spectra using ATR apparatus with 4 1/cm resolution between 4000 and 650 1/cm.

Setaram Labsys Evo Gravimetric Analyzer (TG/DSC 1600 model, France) was processed to describe the thermal behaviors of the composite hydrogels. Approximately 4–6 mg of samples were placed in ceramic crucibles and analyzed during heating up to 50–1000 °C under Argon atmosphere with 100 mL/min flow rate at 10 °C/min heating rate.

Scanning electron microscopy (SEM) of the composite hydrogels was performed to visualize the hydrogel pores. The microstructure of the hydrogel was imaged using an SEM (JOEL JSM 5600, Japan) operated at 20 kV.

Swelling ratio measurements (S) for composite hydrogels were performed out in triplicate at room temperature (%) calculated as

$$S\% = \left(\frac{(M_t - M_0)}{M_0}\right) \times 100, \tag{1}$$

where M_0 and M_t are the initial mass and the mass at time t, respectively. All the experiments were carried out in triplicate and the average values are reported with their standard deviations (Barakat and Sahiner 2008).

Utilization of the Synthesized Composite Hydrogels for Absorption of Some Textile Dyes

The dye absorption experiments were carried out at 25 °C using different dye solutions of TB, AR, and G. The effects of the selected dye concentrations on the absorption performance of the prepared composite hydrogels were investigated by preparing 1 g/L of composite hydrogel solution, while dye concentrations were varied from 10 to 100 mg/L for 24 h. A set of experiment was conducted to determine the contact time on the dye absorption. Additional experiments for the time-dependent absorption were conducted with a constant dye concentration of 10 mg/L at constant composite hydrogels amount of 0.25 g/L and mixing speed of 150 rpm. The samples were withdrawn from the medium at certain time intervals for the measurements. Finally, the dye absorption capacity in pH buffer solutions under experimental conditions as dye concentration 50 mg/L, absorbent dosage 1 g/L, and time 24 h was investigated. In all absorption studies, a UV–Vis spectroscopy was used to quantify absorbed dye amount and analyses for TB, AR, G and dyes were a measurement in the 640, 249, and 610 nm wavenumber, respectively.

The amount of absorbed dye per unit mass of the composite hydrogel, q_e (mg/g) was calculated using the following equation:

$$q_e = \frac{(C_o - C_e) \times V}{W}, \tag{2}$$

where C_o and C_e are the initial and equilibrium dye concentrations (mg/L), respectively, V is the volume of dye solution (L), and W is the weight (g) of the composite hydrogels used.

The removal percentage of dye was calculated as follows (Caria et al. 2009):

$$\text{Removal}\,\% = \frac{(C_o - C_e)}{C_o} \times 100. \tag{3}$$

The processed through Langmuir and Freundlich isotherms (Langmuir 1918; Freundlich 1906) by applying below equations:

$$\frac{C_e}{q_e} = \left(\frac{C_e}{q_{max}}\right) + \left(\frac{1}{q_{max} \times K_L}\right), \tag{4}$$

where q_e is the amount of absorbed dye at equilibrium (mg/g), q_{max} is the maximum absorption capacity of dyes (mg/g), and K_L is the Langmuir absorption equilibrium constant (L/mg). The Langmuir constants, q_{max} and K_L, were determined from the slope and intercept of the linear plot of specific absorptions (C_e/q_e) against the equilibrium concentrations (C_e) for TB, AR, and G dyes:

$$\log\, q_e = \log K_f + \left(\frac{1}{n}\right) \log C_e \tag{5}$$

where K_f and n are the physical Freundlich constants.

The kinetic studies were carried out in accordance with the literature (Lagergren 1898; Blanchard et al. 1984; Namasivayam and Sureshkumar 2008; Ersen Dudu et al. 2015; Gueu et al. 2007). Equations 6 and 7 represent the change of absorption capacity with time for first and second pseudokinetics:

$$\frac{dq_t}{dt} = k_{p1}(q_e - q_t) \tag{6}$$

where q_t(mg/g) is the absorption capacities at time t (min), and k_{p1} (L/min) is the pseudo-first-order rate constant for the kinetic model.

Pseudo-second-order rate kinetic is expressed as

$$\frac{dq_t}{dt} = k_{p2}(q_e - q_t)^2 \tag{7}$$

where k_{p2} (L/min) is the pseudo-second-order rate constant for the kinetic model.

The intra-particle diffusion model can be presented as (Kim et al. 2012; Tian et al. 2011)

$$q_t = R_{id}\sqrt{t} + C \tag{8}$$

where C is the intercept and R_{id} is the rate constant of intra-particle diffusion [mg/(g $h^{1/2}$)].

Results and Discussion

Synthesis and Characterization of the Composite Hydrogels

There are a lot of studies focused on the synthesis of a new class of polymeric materials and their composites which being used for the adsorption of heavy metals, dyes, and several contaminants from aqueous media (Tasdelen et al. 2016; Yu et al. 2016). In the present study, hydrogel–fungus composites were synthesized for the first time and utilized for some dye absorption. AMPS and APTMACl monomers were used as polymeric parts, while *P. squamosus* (Huds.) *Fr.* was used as the bio-part of composite hydrogels. Synthesis and preparation of the composite hydrogels were carried out by modification of related polymerization techniques (Sahiner and Alpaslan 2014; Ersen Dudu et al. 2015).

As the first time, composite hydrogels were synthesized, and the conformation of the functional groups in the composites materials required to be analyzed. Figure 1 represents the FT-IR spectra of the composites materials. The peaks belonging to the AMPS, APTMACl monomers, and crosslinker were at 3432, 3326, 3419, 3305, 3362, and 3246 1/cm, while N–H-stretching vibrations of the secondary amine and a broadening were observed after the addition of *P. squamosus* (Huds.) *Fr.* fungus. Furthermore, the peaks observed at 2934, 2936, and 2946 1/cm in all spectra of the hydrogels belong to –CH-stretching vibrations, while the peaks at 1651, 1644, and 1641 1/cm in the spectra belong to the C=O-stretching vibrations, and peaks at 1455, 1481, and 1479 1/cm in the spectra belong to the C–N stretching vibrations for p(AMPS)-*P. squamosus* (Huds.) *Fr.*, p(AMPS-co-APTMACl)-*P. squamosus* (Huds.) *Fr.*, and p(APTMACl)-*P. squamosus* (Huds.) *Fr.*, respectively. The peak observed at 1179 1/cm of the AMPS monomer belongs to S=O-stretching vibrations of the sulfonic acid. The broad and sharp peaks observed at 1032 and 1081 1/cm can be thought to belong to *P. squamosus* (Huds.) *Fr.* fungus.

The thermal stabilities of the composite hydrogels were investigated by TGA/DSC analyzer and are represented in Fig. 2. As clearly appeared in the figure, the thermal degradation of p(AMPS)-*P. squamosus* (Huds.) *Fr.* composite hydrogel occurred in five steps. At the initial stage, the first mass loss was around 21.9% (265–350 °C) due to evaporation of the water content and some low-weight molecular structures. The second step began when the temperature was in the range of 350–423 °C, while the mass loss in that step was 8.6% approximately. The third step began when the temperature was in the range of 423–686 °C, while the mass loss in that step was about 5.9%. The fourth step began when the temperature was in the range of 686–769 °C, while the mass loss in that step was about 7.9%. The last step began when the temperature was in the range of 769–864 °C and the mass loss was about 4.8%. During all five steps, the thermal decomposition was about 49.1%. As shown in the figure, the thermal degradation of p(AMPS-co-APTMACl)-*P. squamosus* (Huds.) *Fr.* composite hydrogel existed in three steps. At the initial stage, the first mass loss was around 22.7% (274 °C). The second step began when the temperature was in the range of 274–370 °C, while the mass loss in that step was 73.8% approximately. The third step began when the

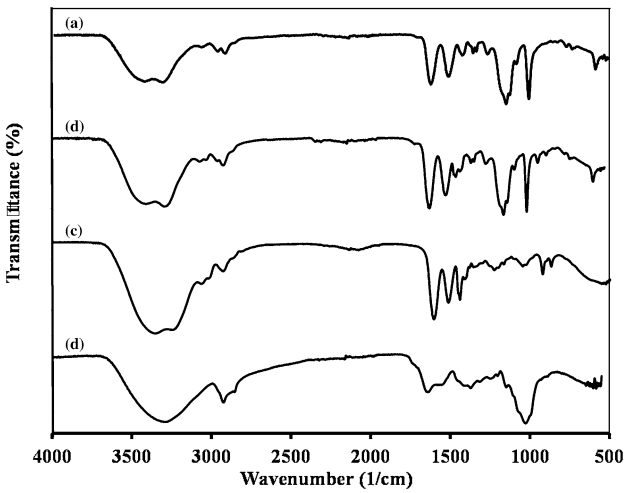

Fig. 1 FT-IR Spectra of **a** p(AMPS)-*P. squamosus* (Huds.) *Fr.*, **b** p(AMPS-co-APTMACl)-*P. squamosus* (Huds.) *Fr.*, **c** p(APTMACl)-*P. squamosus* (Huds.) *Fr.* composite hydrogels, and **d** *P. squamosus* (Huds.) *Fr.* fungus

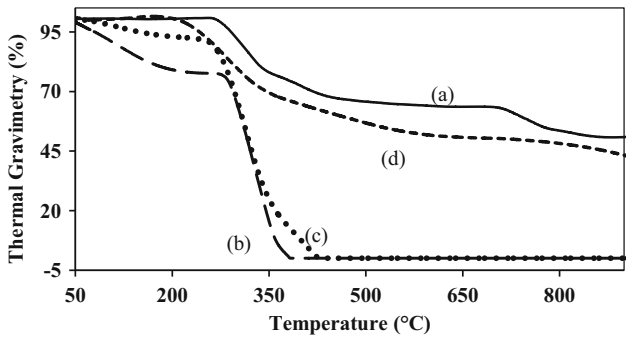

Fig. 2 Thermogarviemtric Analysis of **a** p(AMPS)-*P. squamosus* (Huds.) *Fr.*, **b** p(AMPS-co-APTMACl)-*P. squamosus* (Huds.) *Fr.*, **c** p(APTMACl)-*P. squamosus* (Huds.) *Fr.* composite hydrogels, and **d** *P. squamosus* (Huds.) *Fr.* fungus

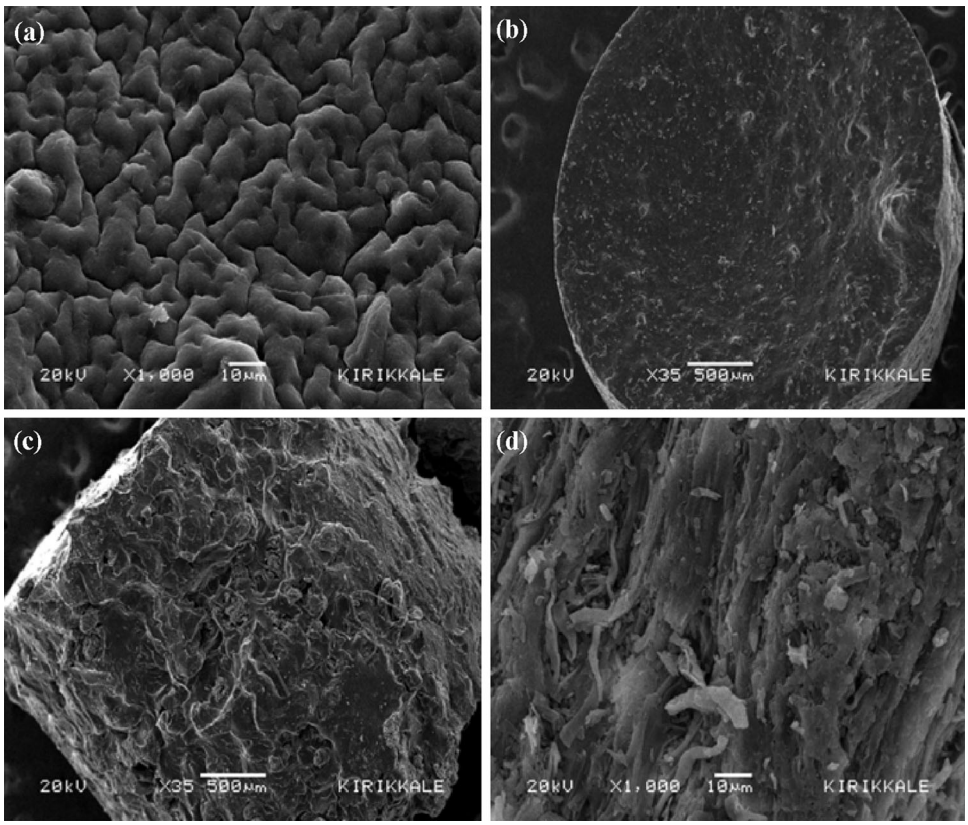

Fig. 3 Scanning Electron Micrographs of **a** p(AMPS)-*P. squamosus* (Huds.) *Fr.*, **b** p(AMPS-co-APTMACl)-*P. squamosus* (Huds.) *Fr.*, **c** p(APTMACl)-*P. squamosus* (Huds.) *Fr.* composite hydrogels, and **d** *P. squamosus* (Huds.) *Fr.* fungus

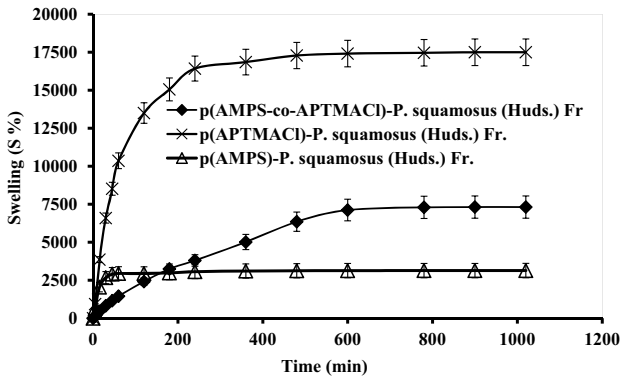

Fig. 4 Percent swelling degree of the p(AMPS-co-APTMACl)-*P. squamosus* (Huds.) *Fr.*, p(APTMACl)-*P. squamosus* (Huds.) *Fr.,* and p(AMPS)-*P. squamosus* (Huds.) *Fr.* composite hydrogels with time in DI water

temperature was in the range of 370–483 °C, while the mass loss in that step inclined to be constant. The total mass loss of p(AMPS-co-APTMACl)-*P. squamosus* (Huds.) *Fr.* composite hydrogel was achieved almost 100% when the temperature rose up to 483 °C. In the second and third steps, the main chains and crosslinked networks of hydrogel were destroyed and weight loss increased. The thermal degradation of p(APTMACl)-*P. squamosus* (Huds.) *Fr*. composite hydrogel was observed in three steps as other composites. As shown in the figure, the first mass loss of composite hydrogel was appeared at 248 °C due to separable water content at the surface and it was approximately 8.4%. The second step began when the temperature was in the range of 248–361 °C, while the mass loss in that step was 71.8% approximately. The mass loss in the last decomposition step was about 19.8% from 361 to 497 °C. The total mass loss of p(APTMACl)-*P. squamosus* (Huds.) *Fr.* composite hydrogel was achieved almost 100% when the temperature rose up to 497 °C. The thermal degradation of *P. squamosus* (Huds.) *Fr.* fungus was in three steps. At the initial stage, the first mass loss began when the temperature was in the range of 176–345 °C, while the mass loss in that step was 29.8% approximately. The second step began when the temperature was in the range of 345–596 °C, while the mass loss in that step was 18.4% approximately. The third step began when the temperature was in the range of 596–951 °C, while the mass loss in that step was about 11.6%. The total mass loss of *P. squamosus* (Huds.) *Fr.* fungus was achieved almost by 59.8% when the temperature rose up to 951 °C.

It was clearly observed from the thermal behavior of that the addition of the fungus to the hydrogel was gained thermal resistance to the composites materials. As the temperature of the p(AMPS-co-APTMACl)-*P. squamosus* (Huds.) *Fr.* and p(APTMACl)-*P. squamosus* (Huds.) *Fr.* composite hydrogels increased, the mass loss also

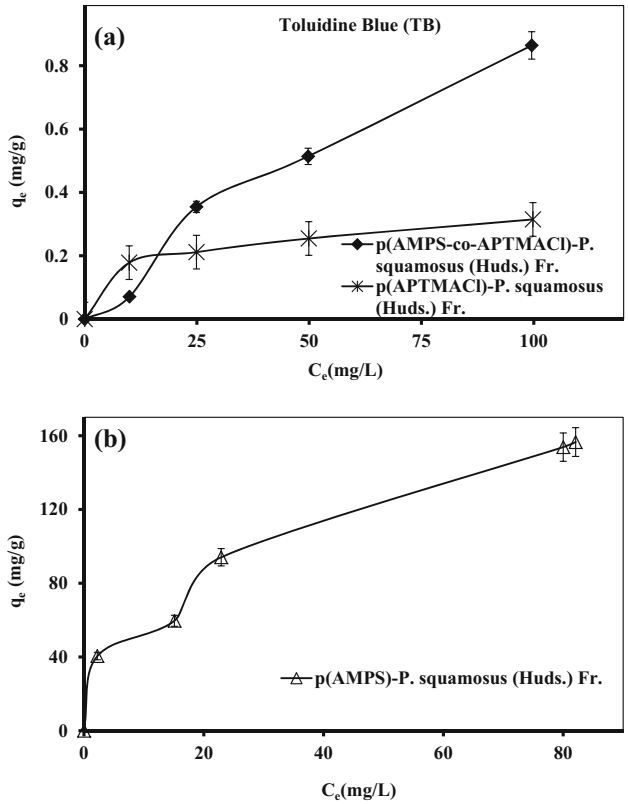

Fig. 5 q_e vs C_e graphs at different Toluidine Blue (TB) concentrations **(a)** of the p(APTMACl-co-AMPS)-*P. squamosus* (Huds.) *Fr.,* and p(APTMACl)-*P. squamosus* (Huds.) *Fr.* composite hydrogels, and **b** of the p(AMPS)-*P. squamosus* (Huds.) *Fr.* composite hydrogels, respectively. [Dye concentration: 10–100 mg/L (50 mL), absorbent dosage: 1 g/L, and time: 24 h]

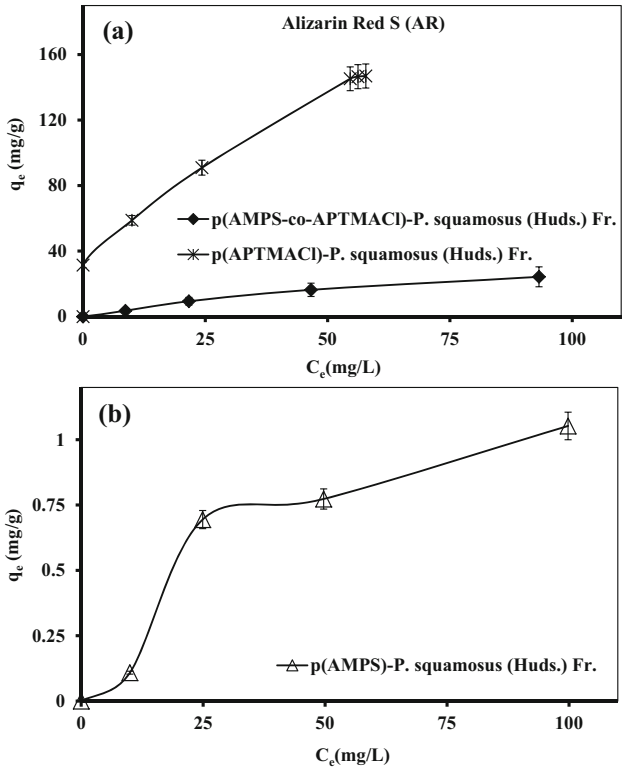

Fig. 6 q_e vs C_e graphs at different Alizarin Red S (AR) concentrations **(a)** of the p(APTMACl-co-AMPS)-*P. squamosus* (Huds.) *Fr.*, and p(APTMACl)-*P. squamosus* (Huds.) *Fr.* composite hydrogels, and **b** of the p(AMPS)-*P. squamosus* (Huds.) *Fr.* composite hydrogels, respectively. [Dye concentration: 10–100 mg/L (50 mL), absorbent dosage: 1 g/L, and time: 24 h]

increased and reached 100%. It was observed that the thermal degradation behavior of the hydrogels changed after the addition of fungus to the structure of the composite hydrogel. The number of degradation step of p(APTMACl)-*P. squamosus* (Huds.) *Fr.* composite hydrogels decreased with increasing in temperature. It was concluded that the there was interaction such as molecular and hydrogen bonds established between fungus and hydrogel (Sahiner et al. 2010, 2015).

SEM images of composite hydrogels were observed and is shown in Fig. 3. As clearly seen in Fig. 3, the surface morphologies of composite hydrogels have undulant and coarse surfaces. Those kinds of surfaces enable relatively long contact and retention time to the aqueous media and sometimes make a local mixing effect to the solution on the composite surface resulted in higher absorption or adsorption of targeted components.

Swelling ratio measurement (S) is important one parameter to explain hydrogel properties such as the types of hydrophilic monomers, composition of the hydrogel, the particle size, and the surface area (Wang and Wang 2009). Figure 4 shows the swelling rate curves of all composite hydrogels in distilled water. All composite hydrogels shown similar swelling behavior and started to reach equilibrium after 360 min. Experiment data demonstrate that the maximum S% degree values were 7120, 17,287, and 3108% for p(AMPS-co-APTMACl)-*P. squamosus* (Huds.) *Fr.*, p(APTMACl)-*P. squamosus* (Huds.) *Fr.,* and p(AMPS)-*P. squamosus* (Huds.) *Fr.* composite hydrogels, respectively. In addition, the swelling degrees of synthesized composite hydrogels were compared with the literature. According to the literature, the swelling values of were reported as about 9048% (Ersen Dudu et al. 2015) for pure p(APTMACl) hydrogel and as about 9000% (Ozay et al. 2009) for pure p(AMPS) hydrogel. The swelling degree of p(AMPS)-*P. squamosus* (Huds.) *Fr.* was relatively low. A decrease in swelling degrees was expected when fungus added to the polymer solution because of the low water absorption of fungus and interplay or bonding and crosslinking density between AMPS and fungus.

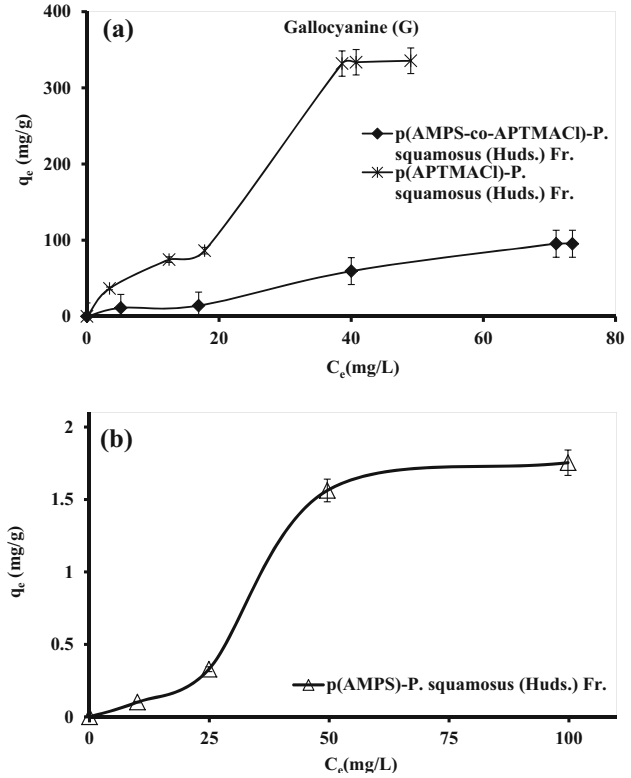

Fig. 7 q_e vs C_e graphs at different Gallocyanine (G) concentrations **(a)** of the p(APTMACl- co-AMPS)-*P. squamosus* (Huds.) *Fr.,* and p(APTMACl)-*P. squamosus* (Huds.) *Fr.* composite hydrogels, and **b** of the p(AMPS)-*P. squamosus* (Huds.) *Fr.* composite hydrogels, respectively. [Dye concentration: 10–100 mg/L (50 mL), absorbent dosage: 1 g/L, and time: 24 h]

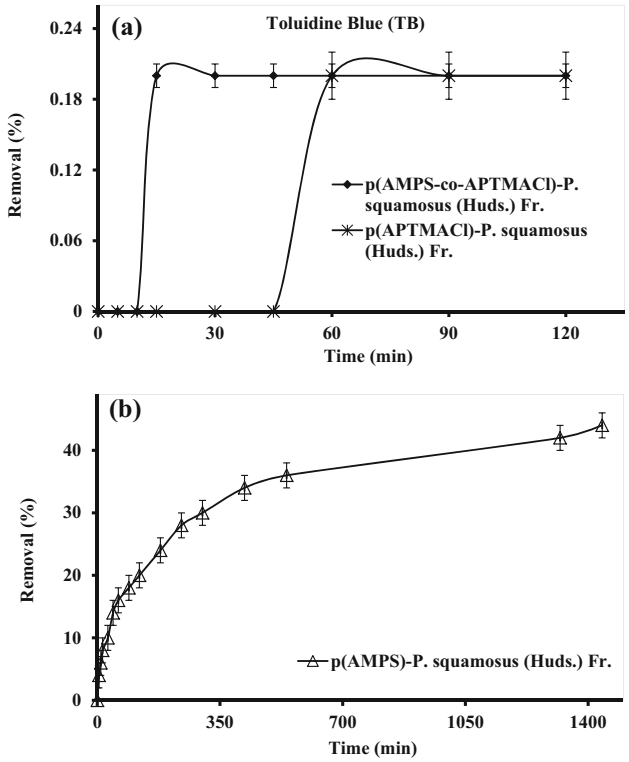

Fig. 8 Effect of contact time on Toluidine Blue (TB) absorption, **a** by the p(APTMACl-co-AMPS)-*P. squamosus* (Huds.) *Fr.*, and p(APTMACl)-*P. squamosus* (Huds.) *Fr.*, and **b** by the p(AMPS)-*P. squamosus* (Huds.) *Fr.* composite hydrogels [Dye concentration: 10 mg/L (50 mL), absorbent dosage: 0.25 g/L]

Utilization of the Synthesized Composite Hydrogels for Absorption of Some Textile Dyes

Both synthesized anionic and cationic composite hydrogels were utilized as absorbents for removal of some dyes such as TB, AR, and G in batch-type absorption studies. The dye concentrations varied from 10 to 100 mg/L, while the composite hydrogel dosage was kept constant at 1 g/L in all experiments. The contact time was extended to 24 h. As shown in Figs. 5, 6, and 7, at low dye/adsorbent ratios, all three dyes were absorbed by the composites. As the dye/adsorbent ratio increased, the higher energy sites are saturated and absorption begins in lower energy sites, resulting in decreases in the absorption efficiency (Bhattacharya et al. 2008). As shown in Fig. 5a, p(APTMACl)-*P. squamosus* (Huds.) *Fr.* and p(AMPS-co-APTMACl)-*P. squamosus* (Huds.) *Fr.* composite hydrogels were non-selective for TB dye due to the ionic character of both composite hydrogels and TB dye. As shown in Fig. 5b, p(AMPS)-*P. squamosus* (Huds.) *Fr.* composite hydrogel, which has an anionic character, showed high selectivity for TB dye, which is cationic. As shown in Figs. 6a and 7a, p(APTMACl)-*P. squamosus* (Huds.) *Fr.*based composites were absorbed AR and G dyes, respectively. The opposite charges of cationic composite hydrogels and anionic dyes forces to absorption positively (Saraydın et al. 2001). In Figs. 6b and 7b observed that of the p(AMPS)-*P. squamosus* (Huds.) *Fr.* composite, hydrogel was non-absorbing of the AR and G dyes. This situation can be defined by the fact that composite hydrogel, AR and G dyes have anionic character. Moreover, in Fig. 7a, the p(AMPS-co-APTMACl)-*P. squamosus* (Huds.) *Fr.* composite hydrogel was shown to have selective behavior towards G dye.

The absorption kinetics of the dyes by composite hydrogels was investigated, and the results are given in Figs. 8, 9, and 10. It is obvious that there is a fast increase in the dye removal, and then, there is a slow-down approaching equilibrium for the studied dyes. In Fig. 8b, maximum dye absorption capacities with time (depending on removal percentage) of p(AMPS)-*P. squamosus* (Huds.) *Fr.* were found as 44% in 1444 min for TB. As shown in Fig. 9a, the highest dye absorption capacities of p(APTMACl)-*P. squamosus* (Huds.) *Fr.* were established as 65.2% in 420 min for AR. According to Fig. 10a, maximum dye absorption of p(APTMACl)-*P. squamosus* (Huds.) *Fr.* was established as 77.3% in 480 min for G.

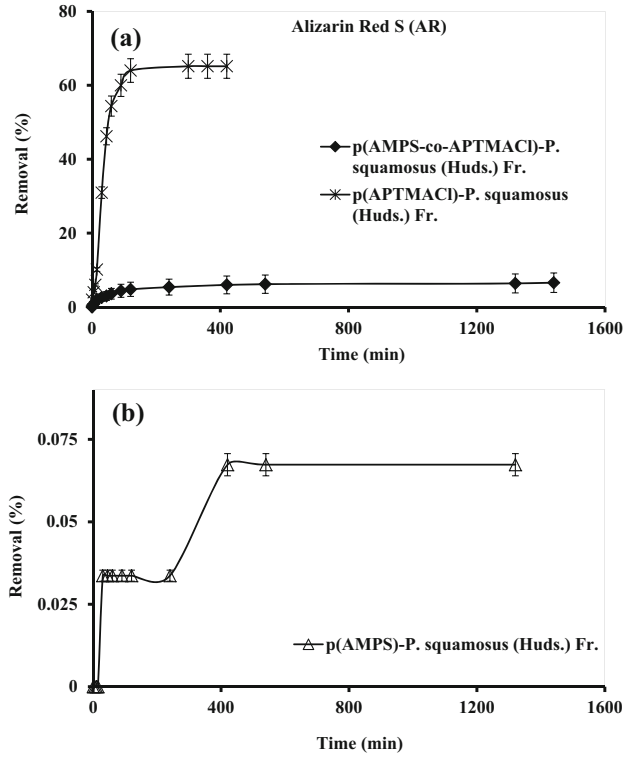

Fig. 9 Effect of contact time on Alizarin Red S (AR) absorption, **a** by the p(APTMACl-co-AMPS)-*P. squamosus* (Huds.) *Fr.,* and p(APTMACl)-*P. squamosus* (Huds.) *Fr.,* and **b** by the p(AMPS)-*P. squamosus* (Huds.) *Fr.* composite hydrogels [Dye concentration: 10 mg/L (50 mL), absorbent dosage: 0.25 g/L]

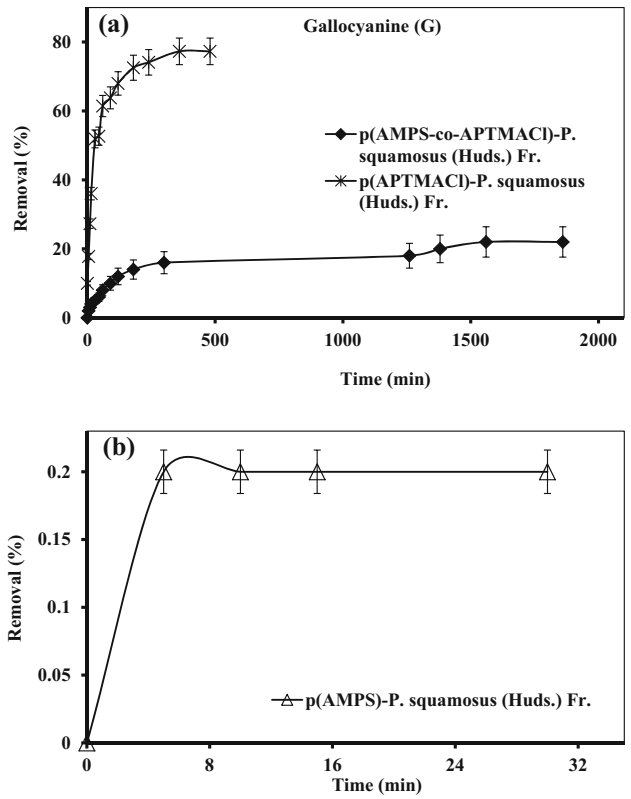

Fig. 10 Effect of contact time on Gallocyanine (G) absorption, **a** by the p(APTMACl-co-AMPS)-*P. squamosus* (Huds.) *Fr.,* and p(APTMACl)-*P. squamosus* (Huds.) *Fr.*, and **b** by the p(AMPS)-*P. squamosus* (Huds.) *Fr.* composite hydrogels [Dye concentration: 10 mg/L (50 mL), absorbent dosage: 0.25 g/L]

It is well known that the pH significantly affects adsorption capacity of any kind of adsorbents, since the surface charge of an absorbent, and the ionization behavior of absorbents and dyes varies in the medium pH (Li et al. 2013). Table 1 indicates the removal percentage of dyes by composite hydrogels over a pH range of 2–10. In those experiments, 50 mg/L of the prepared dyes solutions were used. As shown in Table 1, the removal of the dyes was significantly affected by medium pH. The highest absorption capability of the TB dye was reached at a maximum level as 73.2% at pH 8 for the p(AMPS)-*P. squamosus* (Huds.) *Fr.* The increase of TB absorption onto p(AMPS)-*P. squamosus* (Huds.) *Fr.* with increasing pH values can be explained by the electrostatic interaction between cationic dye and negatively charged AMPS surface (Alpat et al. 2008). In addition, the highest absorption capability of the G dye was observed to be 69.4% at pH 6 for the p(APTMACl)-*P. squamosus* (Huds.) *Fr.*-based composites hydrogels. As shown, the highest absorption capability of AR dye reached 43.6% at pH 6 for the p(APTMACl)-*P. squamosus* (Huds.) *Fr.* Since AR is an anionic dye, it is conceivable that at low pH, its absorption is favored on a positively charged surface. In principle, when the zero point charge (pH_{zpc}) of APTMACl was low from solution pH, at pH < pH_{zpc}, the surface becomes positively charged and favors the uptake of anionic dye to increased electrostatic force of attraction (Gautam et al. 2013).

Absorption Isotherm Studies

Both Langmuir and Freundlich absorption isotherms were considered to be the most utilized ones for ea physicochemical approach using for modeling of the equilibrium data (Langmuir 1918; Freundlich 1906). The corresponding isotherms were formed for TB, AR, and G dye absorptions by composite hydrogels by applying Langmuir and Freundlich equations. The data are given in Table 2. Freundlich isotherm equation, which is an empirical equation, was applied the selected ions absorption by composite hydrogels and the values of K_f and n are calculated from the intercept and slope of the plot of log C_e against logq_e (Langmuir 1918; Freundlich 1906; Namasivayam and Sureshkumar 2008; Alpaslan et al. 2014; Ersen Dudu et al. 2015). If a value for n is equal to unity, the absorption is linear. If a value for n is below to unity, the absorption is unfavorable, but the magnitude value of

Table 1 Absorption of TB, AR, and G dyes into composite hydrogels as a function of solution pH

Composite hydrogels	Dyes	pH	Minimum removal (%)	pH	Maximum removal (%)
p(AMPS-co-APTMACl)-*P. squamosus* (Huds.) *Fr.*	TB	2	0.2	6	0.8
p(APTMACl)-*P. squamosus* (Huds.) *Fr.*		8	0.2	4	6.4
p(AMPS)-*P. squamosus* (Huds.) *Fr.*		2	20.2	8	73.2
p(AMPS-co-APTMACl)-*P. squamosus* (Huds.) *Fr.*	AR	2	0.2	10	0.2
p(APTMACl)-*P. squamosus* (Huds.) *Fr.*		2	0.2	6	43.6
p(AMPS)-*P. squamosus* (Huds.) *Fr.*		2	0.2	10	0.2
p(AMPS-co-APTMACl)-*P. squamosus* (Huds.) *Fr.*	G	10	0.2	6	28
p(APTMACl)-*P. squamosus* (Huds.) *Fr.*		2	13.8	6	69.4
p(AMPS)-*P. squamosus* (Huds.) *Fr.*		2	0.2	8	0.6

[Dye concentration: 50 mg/L (50 mL), absorbent dosage: 1 g/L, time: 24 h]

Table 2 Langmuir and Freundlich isotherm data for absorption of TB, AR, and G dyes by composite hydrogels

Composite Hydrogels	Dyes	Langmuir isotherm constants			Freundlich isotherm constants		
		K_L (L/mg)	q_m (mg/g)	R^2	K_f	n	R^2
p(AMPS-co-APTMACl)-*P. squamosus* (Huds.) *Fr.*	TB	1.1×10^{-2}	0.9	0.6241	8.9×10^{-3}	0.9	0.9365
p(APTMACl)-*P. squamosus* (Huds.) *Fr.*		1.3×10^{-2}	0.5	0.7225	9.8×10^{-2}	3.9	0.9886
p(AMPS)-*P. squamosus* (Huds.) *Fr.*		0.5×10^{-1}	188.7	0.9478	26.8	2.6	0.9415
p(AMPS-co-APTMACl)-*P. squamosus* (Huds.) *Fr.*	AR	1.32×10^{-2}	1.8	0.6916	7.2×10^{-1}	1.3	0.9823
p(APTMACl)-*P. squamosus* (Huds.) *Fr.*		8.75×10^{-2}	140.9	0.8997	60.9	6.1	0.8316
p(AMPS)-*P. squamosus* (Huds.) *Fr.*		5.55×10^{-3}	3.1	0.2667	2.2×10^{-2}	1.2	0.8467
p(AMPS-co-APTMACl)-*P. squamosus* (Huds.) *Fr.*	G	3.95×10^{-4}	3333.3	0.0016	2.0	1.1	0.9078
p(APTMACl)-*P. squamosus* (Huds.) *Fr.*		-1.23×10^{-2}	− 277.8	0.6299	9.3	1.1	0.9040
p(AMPS)-*P. squamosus* (Huds.) *Fr.*		-4.04×10^{-3}	− 2.5	0.7869	6.3×10^{-3}	0.8	0.9345

$n > 1$ indicates that the absorption was favorable (Hameed et al. 2008; Selvam et al. 2008).

Table 2 shows the data of Langmuir and Freundlich isotherms' constants for composite hydrogels. Comparison of both theoretical isotherms used in this study shows that the Freundlich equation generally fits the experimental data in a better. The values of the correlation coefficients indicate the favorable nature of absorption of the dyes on composite hydrogels. The absorption intensity given by the Freundlich coefficient, $n > 1$, is relatively favorable for all dye forms absorption. In addition, if a value for Langmuir constant is below zero, this isotherm is known to be unfavorable for the absorption process (Akgöl et al. 2006; Selvam et al. 2008).

A well comparison of the data obtained during this study and those of the literature are given in Table 3. It is indicated that absorption capacities of composite hydrogels are very well when compared to those of the literature (Aksu and Karabayır 2008; Alpat et al. 2008; Fan et al. 2012; Gautam et al. 2013; Karadağ et al. 2002; Maurya and Mittal 2008; Tunc et al. 2009; Zolgharnein et al. 2014a, b).

Absorption Reaction Models

The absorption kinetics of different dyes by composite hydrogels was studied. The rate of the absorption of the selected dye on composite hydrogels was analyzed with three kinetic models which are pseudofirst order, pseudosecond order, and intra-particle diffusion. The similarity between experimental data and the model-predicted values was denoted by the correlation coefficients (R^2), as shown in Table 4. A relatively high R^2 value proves that the model successfully defines the kinetics of dye absorption (Yagub et al. 2014; Kumar et al. 2010; Lakshmi et al. 2009). The pseudofirst- and second-order plots of $\log(q_e - q_t)$ vs t (min) and t/q_t against t for the selected dyes absorption by cationic or anionic hydrogels were plotted, and K_{p1}, K_{p2} and q_e were determined from the slope and intercept of plot, as given in Tables 4 and 5. As comparing R^2; R^2 for the pseudofirst-order kinetics indicated better suitability fitted all dye forms absorption for the all composite hydrogels excepted TB dye absorption for the p(AMPS)-*P. squamosus* (Huds.) *Fr.* hydrogels. Furthermore, R^2 values led to the conclusion that the

Table 3 Comparison of absorption or adsorption capacity of some similar absorbents appeared in the literature

Absorbents	Dyes	Absorption or adsorption (mg/g)	References
Magnetic chitosan	AR	40.1	Fan et al. (2012)
Mustard husk	AR	6.1	Gautam et al. (2013)
Nano γ-alumina	AR	51.4	Zolgharnein et al. (2014a)
CTAB-modified TiO_2 nanoparticles (single)	AR	30.9	Zolgharnein et al. (2014b)
CTAB-modified TiO_2 nanoparticles (binary)	AR	20.7	Zolgharnein et al. (2014b)
Turkish zeolite	TB (or TBO)	27.5	Alpat et al. (2008)
Acrylamide (Aam)/maleic Acid (MA) hydrogels	TB	3.4	Karadağ et al. (2002)
Rhizopus arrhizus	Gryfalan black RL	590.8	Aksu and Karabayır (2008)
Trametes versicolor	Gryfalan black RL	370.3	Aksu and Karabayır (2008)
Aspergillus niger	Gryfalan black RL	282.7	Aksu and Karabayır (2008)
Cotton stalk	Remazol black B	34.1	Tunc et al. (2009)
Fomitopsis carnea (KL)	G	115	Maurya and Mittal (2008)
Fomentarius (BM)	G	98.8	Maurya and Mittal (2008)
p(AMPS)-*P. squamosus* (Huds.) *Fr.*	TB	156.6	This work
p(AMPS-co-APTMACl)-*P. squamosus* (Huds.) *Fr.*	TB	0.86	This work
p(APTMACl)-*P. squamosus* (Huds.) *Fr.*	TB	0.32	This work
p(APTMACl)-*P. squamosus* (Huds.) *Fr.*	AR	147	This work
p(AMPS-co-APTMACl)-*P. squamosus* (Huds.) *Fr.*	AR	24.3	This work
p(AMPS)-*P. squamosus* (Huds.) *Fr.*	AR	1.1	This work
p(APTMACl)-*P. squamosus* (Huds.) *Fr.*	G	335.6	This work
p(AMPS-co-APTMACl)-*P. squamosus* (Huds.) *Fr.*	G	95.4	This work
p(AMPS)-*P. squamosus* (Huds.) *Fr.*	G	1.7	This work

Table 4 Kinetic constants for absorption of TB, AR, and G dyes by composite hydrogels

Composite hydrogels	Dyes	Pseudofirst order		Pseudosecond order		Intra-particle diffusion	
		K_{p1} (L/min)	R^2	K_{p2} [g/(mg min)]	R^2	R_{id} [mg/(g $min^{1/2}$)]	R^2
p(AMPS-co-APTMACl)-*P. squamosus* (Huds.) *Fr.*	TB	-1.6×10^{-1}	0.6000	–	1.000	1.7×10^{-2}	0.6540
p(APTMACl)-*P. squamosus* (Huds.) *Fr.*		-4.2×10^{-2}	0.5422	5.2×10^{-1}	0.9801	1.1×10^{-2}	0.6969
p(AMPS)-*P. squamosus* (Huds.) *Fr.*		2.9×10^{-3}	0.9712	1.7×10^{-4}	0.9581	1.4	0.9834
p(AMPS-co-APTMACl)-*P. squamosus* (Huds.) *Fr.*	AR	3.5×10^{-3}	0.9655	5.5×10^{-3}	0.9963	8.3×10^{-2}	0.9128
p(APTMACl)-*P. squamosus* (Huds.) *Fr.*		1.3×10^{-2}	0.7810	5.4×10^{-4}	0.9501	3.4	0.8714
p(AMPS)-*P. squamosus* (Huds.) *Fr.*		1.8×10^{-3}	0.8272	6.8×10^{-2}	0.8834	2.4×10^{-3}	0.8368
p(AMPS-co-APTMACl)-*P. squamosus* (Huds.) *Fr.*	G	3.9×10^{-3}	0.9843	8.8×10^{-4}	0.9760	0.4	0.9785
p(APTMACl)-*P. squamosus* (Huds.) *Fr.*		1.2×10^{-2}	0.9460	1.6×10^{-3}	0.9985	1.4	0.8671
p(AMPS)-*P. squamosus* (Huds.) *Fr.*		7.8×10^{-2}	0.3810	7.2×10^{-1}	0.9973	1.2×10^{-2}	0.7271

intra-particle diffusion model was effective on the dye absorption by all the composite hydrogels, as given in Table 4. Table 4 shows that the intra-particle diffusion model plots did not cross the origin demonstrating that both boundary layer diffusion steps and intra-particle diffusion steps are effective in the absorption mechanism (figure not shown). Higher values of R_{id}, which were calculated from Eq. 8, illustrate an enhancement in the rate of absorption, whereas larger R_{id} values illustrate a better absorption mechanism (Sharma and Goyal 2009; Mane et al. 2007; Alpat et al. 2008). In addition, data given in Table 5 indicate that there were no large differences between the experimental $q_{e,exp}$ and the calculated $q_{e,cal}$. In addition, the $q_{e,cal}$ values calculated from pseudofirst-order model were generally more consistent with the experimental $q_{e,exp}$.

Table 5 Absorption capacity of absorption of TB, AR, and G dyes by composite hydrogels

Composite hydrogels	Dyes	Pseudofirst order		Pseudosecond order
		$q_{e,\ exp}$ (mg/g)	$q_{e,\ cal}$ (mg/g)	$q_{e,\ cal}$ (mg/g)
p(AMPS-co-APTMACl)-*P. squamosus* (Huds.) *Fr.*	TB	0.1	0.04	0.1
p(APTMACl)-*P. squamosus* (Huds.) *Fr.*		0.2	0.03	0.1
p(AMPS)-*P. squamosus* (Huds.) *Fr.*		40.9	33.6	44.4
p(AMPS-co-APTMACl)-*P. squamosus* (Huds.) *Fr.*	AR	3.6	2.3	3.6
p(APTMACl)-*P. squamosus* (Huds.) *Fr.*		31.3	19.02	35.9
p(AMPS)-*P. squamosus* (Huds.) *Fr.*		0.1	0.1	0.1
p(AMPS-co-APTMACl)-*P. squamosus* (Huds.) *Fr.*	G	10.8	9.2	11.8
p(APTMACl)-*P. squamosus* (Huds.) *Fr.*		36.7	21.3	37.9
p(AMPS)-*P. squamosus* (Huds.) *Fr.*		0.1	0.4	0.1

Conclusions

Natural, cheap, environmentally friendly, and selective composite-based hydrogels and fungus were fabricated, characterized, and utilized for removal of some textile dyes such as TB, AR, and G. The anionic and cationic hydrogels were synthesized from AMPS, APTMACl via redox polymerization technique, and *P. squamosus* (Huds.) *Fr.* fungus utilized as bio-part. It was observed that the thermal degradation steps of the composite hydrogels changed after the addition fungus to the hydrogels. SEM images reviled that the surface of the fungus–hydrogel composites is rough which enable better absorption for dyes. Freundlich isotherm equation showed the best fit for TB, AR, and G dyes. The absorption behaviors of all dye forms were generally fitted well into a pseudosecond-order kinetic model except the TB dye absorption for the p(AMPS)-*P. squamosus* (Huds.) *Fr.* composite. The maximum absorption capacities of p(AMPS)-*P. squamosus* (Huds.) *Fr.*, p(APTMACl)-*P. squamosus* (Huds.) *Fr.,* and p(APTMACl)-*P. squamosus* (Huds.) *Fr.* composite hydrogels were 40.9 mg/g for TB dye, 31.3 mg/g for AR dye, and 36.7 mg/g for G dye, respectively. It was concluded that prepared hydrogel fungus composites can be considered as absorbents for removal of textile dyes from aqueous media due to its cost, easy preparations, and non-toxic properties.

References

Akbari M, Hallajisani A, Keshtkar AR, Shahbeig H, Ghorbanian SA (2015) Equilibrium and kinetic study and modeling of Cu(II) and Co(II) synergistic biosorption from Cu(II)-Co(II) single and binary mixtures on brown algae *C. indica*. J Environ Chem Eng 3:140–149

Akgöl S, Kuşvuran E, Kara A, Senel S, Denizli A (2006) Porous dye affinity beads for nickel adsorption from aqueous solutions: a kinetic study. J Appl Polym Sci 100:5056–5065

Aksu Z, Karabayır G (2008) Comparison of biosorption properties of different kinds of fungi for the removal of Gryfalan Black RL metal-complex dye. Bioresour Technol 99:7730–7741

Al-Degs YS, El-Barghouthi MI, El-Sheikh AH, Walker GM (2008) Effect of solution pH, ionic strength, and temperature on adsorption behavior of reactive dyes on activated carbon. Dyes Pigment 77:16–23

Alpaslan D, Aktas N, Yilmaz S, Sahiner N, Guven O (2014) The preparation of p (acrylonitrile-co-acrylamide) hydrogels for uranyl ion recovery from aqueous environments. Hacet J Biol Chem 42:89–97

Alpat SK, Ozbayrak O, Alpat S, Akçay H (2008) The adsorption kinetics and removal of cationic dye, Toluidine Blue O, from aqueous solution with Turkish zeolite. J Hazard Mater 151:213–220

Barakat MA, Sahiner N (2008) Cationic hydrogels for toxic arsenate removal from aqueous environment. J Environ Manag 88:955–961

Bhattacharya AK, Naiya TK, Mandal SN, Das SK (2008) Absorption kinetics and equilibrium studies on removal of Cr(VI) from aqueous solutions using different low-cost adsorbent sing. Chem Eng J 137:529–541

Blanchard G, Maunaye M, Martin G (1984) Removal of heavy metals from waters by means of natural zeolites. Water Res 18:1501–1507

Caria G, Alzari V, Monticelli O, Nuvoli D, Kenny JM, Mariani A (2009) Poly(N,*N*-dimethylacrylamide) hydrogels obtained by frontal polymerization. J Polym Sci, Part A: Polym Chem 47:1422–1428

Dong K, Qiu F, Guo X, Xu J, Yang D, He K (2013) Adsorption behavior of azo dye eriochrome black T from aqueous solution by β-cyclodextrins/polyurethane foam material. Polym Plast Technol Eng 52:452–460

Ersen Dudu T, Sahiner M, Alpaslan D, Demirci S, Aktas N (2015) Removal of As (V), Cr(III) and Cr(VI) from aqueous environments by poly (acrylonitril-co-acrylamidopropyl-trimethyl ammonium chloride)-based hydrogels. J Environ Manag 161:243–251

Fan L, Zhang Y, Li X, Luo C, Lu F, Qiu H (2012) Removal of alizarin red from water environment using magnetic chitosan with Alizarin Red as imprinted molecules. Coll Surf B Biointerfaces 91:250–257

Freundlich HMF (1906) Uber die adsorption in losungen. Z Physikalische Chemi 57:385–470

Gautam RK, Mudhoo A, Chattopadhyaya MC (2013) Kinetic, equilibrium, thermodynamic studies and spectroscopic analysis of Alizarin Red S removal by mustard husk. J Environ Chem Eng 1:1283–1291

Gueu S, Yao B, Adouby K, Ado G (2007) Kinetics and thermodynamics study of lead adsorption on to activated carbons from coconut and seed hull of the palm tree. Int J Environ Sci Technol 4:11–17

Hameed BH, Mahmoud DK, Ahmad AL (2008) Equilibrium modeling and kinetic studies on the Absorption of basic dye by a low-cost adsorbent: coconut (Cocos nucifera) bunch waste. J Hazard Mater 158:65–72

Ho YS, McKay G (1999) Pseudo-second order model for sorption processes. Proc Biochem 34:451–465

Iyer A, Mody K, Jha B (2005) Biosorption of heavy metals by a marine bacterium. Marine Poll Bull 50:340–343

Jeon YS, Lei J, Kim JH (2008) Dye adsorption characteristics of alginate/polyaspartate hydrogels. J Ind Eng Chem 14:726–731

Karadağ E, Uzüm OB, Saraydin D (2002) Swelling equilibria and dye adsorption studies of chemically crosslinked superabsorbent acrylamide/maleic acid hydrogels. Eur Polym J 38:2133–2141

Kim YS, Kim DH, Yang JS, Baek K (2012) Adsorption characteristics of As(III) and As(V) on alum sludge from water purification facilities. Sep Sci Technol 47:2211–2217

Kumar PS, Ramalingam S, Senthamarai C, Niranjanaa M, Vijayalakshmi P, Sivanesan S (2010) Adsorption of dye from aqueous solution by cashew nut shell: studies on equilibrium isotherm, kinetics and thermodynamics of interactions. Desalination 261:52–60

Lagergren S (1898) Zur theorie der sogenannten adsorption geloester stoffe. Kungliga Svenska Vetenskapsa. Handlingar 24:1–39

Lakshmi UR, Srivastava VC, Mall ID, Lataye DH (2009) Rice husk ash as an effective adsorbent: evaluation of adsorptive characteristics for Indigo Carmine dye. J Environ Manag 90:710–720

Langmuir I (1918) The adsorption of gases on plane surfaces of glass, mica and platinum. J Am Chem Soc 40:1361

Li Y, Du Q, Liu T, Peng X, Wang J, Sun J, Wang Y, Wu S, Wang Z, Xia Y, Xia L (2013) Comparative study of methylene blue dye adsorption onto activated carbon, graphene oxide, and carbon nanotubes. Chem Eng Res Des 91:361–368

Mahanta D, Madras G, Radhakrishnan S, Patil S (2008) Adsorption of sulfonated dyes by polyaniline emeraldine salt and its kinetics. J Phys Chem B 112:10153–10157

Mane VS, Mall ID, Srivastava VC (2007) Kinetic and equilibrium isotherm studies for the adsorptive removal of Brilliant Green dye from aqueous solution by rice husk ash. J Environ Manag 84:390–400

Maurya NS, Mittal AK (2008) Selection of biosorbent: a case of dyes sorption. Nat Acad Sci Lett 31:221–227

Namasivayam C, Sureshkumar MV (2008) Removal of chromium(VI) from water and wastewater using surfactant modified coconut coir pith as a biosorbent. Bioresour Technol 99:2218–2225

Ozay O, Ekici S, Baran Y, Aktas N, Sahiner N (2009) Removal of toxic metal ions with magnetic hydrogels. Water Research 43: 4403-

Ozay O, Ekici S, Aktas N, Sahiner N (2011) P(4-vinyl pyridine) hydrogel use for the removal of UO_2^{2+} and Th^{4+} from aqueous environments. J Environ Manag 92:3121–3129

Pal A, Ghosh S, Paul AK (2006) Biosorption of cobalt by fungi from serpentine soil of Andaman. Bioresour Technol 97:1253–1258

Sahiner N (2009) A facile method for the preparation of poly(4-vinylpyridine) nanoparticles and their characterization. Turk J Chem 33:23–31

Sahiner N, Alpaslan D (2014) Metal-ion-containing ionic liquid hydrogels and their application to hydrogen production. J Appl Polym Sci. doi:10.1002/APP.40183

Sahiner N, Godbey WT, McPherson GL, John VT (2006) Microgel, nanogel and hydrogel–hydrogel semi-IPN composites for biomedical applications: synthesis and characterization. Coll Polym Sci 284:1121–1129

Sahiner N, Ozay H, Ozay O, Aktas N (2010) A soft hydrogel reactor for cobalt nanoparticle preparation and use in the reduction of nitrophenols. Appl Catal B Environ 101:137–143

Sahiner N, Ozay O, Aktas N (2011) Aromatic organic contaminant removal from an aqueous environment by p (4-VP)-based materials. Chemosphere 85:832–838

Sahiner M, Butun S, Alpaslan D, Bitlisli BO (2014) Preparation of collagen based composite materials with synthetic polymers for potential wound dressing applications. Hacet J Biol Chem 42:63–69

Sahiner N, Demirci S, Sahiner M, Yilmaz S, Al-Lohedan H (2015) The use of superporous p(3-acrylamidopropyl)trimethyl ammonium chloride cryogels for removal of toxic arsenate anions. J Environ Manag 152:66–74

Santhy K, Selvapathy P (2006) Removal of reactive dyes from wastewater by adsorption on coir pith activated carbon. J Bioresour Technol 97:1329–1336

Saraydın D, Karadag E, Güven O (2001) Use of Superswelling Acrylamide/Maleic Acid Hydrogels for Monovalent Cationic Dye Adsorption. J Appl Polym Sci 79:1809–1815

Selvam PP, Preethi S, Basakaralingam P, Thinakaran N, Sivasamy A, Sivanesan S (2008) Removal of rhodamine B from aqueous solution by adsorption onto sodium montmorillonite. J Hazard Mater 155:39–44

Sharma I, Goyal D (2009) Kinetic modeling: chromium(III) removal from aqueous solution by microbial waste biomass. J Sci Ind Res 68:640–646

Soylak M, Tuzen M, Mendil D, Turkekul I (2006) Biosorption of heavy metals on Aspergillus fumigatus immobilized Diaion HP-2MG resin for their atomic absorption spectrometric determinations. Talanta 70:1129–1135

Tasdelen B, Izlen Cifci D, Meric S (2016) Preparation of N-isopropylacrylamide/itaconic acid/Pumice highly swollen composite hydrogels to explore their removal capacity of methylene blue Physicochemical and Engineering Aspects. Coll Surf A. doi:10.1016/j.colsurfa.2016.11.003

Tian G, Geng J, Jin Y, Wang C, Li S, Chen Z, Wang H, Zhao Y, Li S (2011) Sorption of uranium(VI) using oxime-grafted ordered mesoporous carbon CMK-5. J Hazard Mater 190:442–450

Tunc O, Tanacı H, Aksu Z (2009) Potential use of cotton plant wastes for the removal of Remazol Black B reactive dye. J Hazard Mater 163:187–198

Vijayaraghavan K, Jegan J, Palanivelu K, Velan M (2005) Biosorption of cobalt(II) and nickel(II) by seaweeds: batch and column studies. Sep Purif Technol 44:53–59

Wang W, Wang A (2009) Synthesis, swelling behaviors, and slow-release characteristics of a guar gum-g-poly(sodium acrylate)/sodium humate superabsorbent. J Appl Polym Sci 112:2102–2111

Wang HL, Li P, Liu GS, Li X, Yao JM (2010) Rapid biodecolourization of eriochrome black T wastewater by bioaugmented aerobic granules cultivated through a specific method. Enzyme Microb Technol 47:37–43

Yagub MT, Sen TK, Afroze S, Ang HM (2014) Dye and its removal from aqueous solution by adsorption: a review. Adv Coll Interface Sci 209:172–184

Yu C, Wang F, Zhang C, Fu S, Lucia LA (2016) The synthesis and absorption dynamics of a lignin-based hydrogel for remediation of cationic dye-contaminated effluent. React Funct Polym 106:137–142

Zolgharnein J, Asanjrani N, Bagtash M, Azimi G (2014a) Multi-response optimization using Taguchi design and principle component analysis for removing binary mixture of alizarin red and alizarin yellow from aqueous solution by nano γ-alumina. Spectrochim Acta Part A Mol Biomol Spectrosc 126:291–300

Zolgharnein J, Bagtash M, Asanjarani N (2014b) Hybrid central composite design approach for simultaneous optimization of removal of Alizarin Red S and Indigo Carmine dyes using cetyltrimethylammonium bromide-modified TiO_2 nano-particles. J Environ Chem Eng 2:988–1000